nature communications

Article

https://doi.org/10.1038/s41467-026-68776-8

Stereoselective cyano translocation reaction enabled by photoenzymatic catalysis

Received: 9 September 2025

Accepted: 16 January 2026

Published online: 29 January 2026

Check for updates

Xinyu Duan[1,3], Jie Xu[1,3], Rulin Bai[1,3], Chenlu Jin[1], Yuchen Chu[1], Guojing Wu[1], Liangliang Pan[1], Chunlei Yang[1] ✉, Zhiguo Wang[2] ✉ & Jian Xu[1] ✉

Functional-group translocation constitutes a powerful strategy in organic synthesis, allowing precise modification of molecular architectures and functional group positions. Nevertheless, methodologies capable of delivering precise stereocontrol during such migrations remain exceedingly scarce. Herein, we present a photoenzymatic strategy for cyano translocation that achieves precise stereocontrol. The use of stereo-complementary enzymes grants access to both enantiomers, while mechanistic studies and molecular dynamics simulations delineate the origin of stereoselectivity. This work expands the paradigm of transformations that can be rendered asymmetric by photoenzymatic catalysis and provides a new strategy to tackle persistent challenges in organic synthesis.

Functional groups (FGs) govern the properties and functions of organic molecules, making their introduction, removal, or rearrangement fundamental in organic chemistry[1,2]. Functional-group translocation enables precise modulation of molecular architecture and FG positioning, with profound effects on biological activity and physicochemical properties, thereby expanding the chemical space for drug discovery and materials design[3]. In recent years, significant progress has been made in the development of radical-mediated migratory processes for key functional groups (FGs), such as aryl, alkynyl, acyloxy, hydroxyl, and cyano groups (CN), in which chemoselectivity and regioselectivity are generally well controlled[4–11]. Nevertheless, stereocontrol in these reactions has typically relied on chiral substrates, and the direct achievement of precise stereochemical control remains an unresolved challenge (Fig. 1a)[12].

Biocatalysis has garnered significant attention in synthesis for its mild, environmentally friendly conditions and inherent stereocontrol[13–22]. Recently, the incorporation of classical reactive intermediates into enzyme active sites has enabled the development of new-to-nature reactions, particularly those involving highly reactive intermediates such as carbenes and radicals [23–28], thereby broadening the synthetic potential of enzymatic catalysis. Flavin-dependent enzymes represent one of the most prevalent classes of enzymes in nature, orchestrating a broad spectrum of biological redox transformations[29]. These enzymes facilitate processes including substrate dehydrogenation, monooxygenation, cyclization, and intricate radical-mediated reactions, thereby playing central roles in energy metabolism, signal transduction, and the biosynthesis of diverse natural products[30]. Flavins exhibit exceptional versatility due to their ability to adopt multiple redox states, including oxidized, single-electron reduced, and two-electron reduced forms[31–37]. Recent developments have harnessed photoexcitation to enhance their redox capabilities, enabling radical-mediated coupling reactions with precise stereochemical control[38–47]. Flavin-dependent photoenzymatic catalysis typically proceeds through radical addition to alkenes[38,39]. More recently, the reaction paradigm has been extended to radical additions to nitro compounds[41] and oximes[48], as well as radical-mediated 1,5-hydrogen atom transfer (1,5-HAT) reactions (Fig. 1b)[49]. Nevertheless, alternative pathways within this enzymatic class remain largely unexplored.

We aimed to exploit flavin-dependent enzymes to catalyze stereoselective functional group translocation reactions. Alkyl nitriles are highly valuable synthetic intermediates, as they can be readily transformed into carboxylic acids, amines, and numerous other functional molecules[50–52]. Consequently, the development of enantioenriched alkyl nitriles is of considerable significance in both academia and industry.

[1]Zhejiang Key Laboratory of Bioorganic Synthesis, State Key Laboratory of Green Chemical Synthesis and Conversion, College of Biotechnology and Bioengineering, Zhejiang University of Technology, Hangzhou, PR China. [2]Institute of Ageing Research, School of Basic Medical Sciences, Hangzhou Normal University, Hangzhou, PR China. [3]These authors contributed equally: Xinyu Duan, Jie Xu, Rulin Bai. ✉e-mail: chunleiyang@zjut.edu.cn; zhgwang@aliyun.com; jianxu@zjut.edu.cn

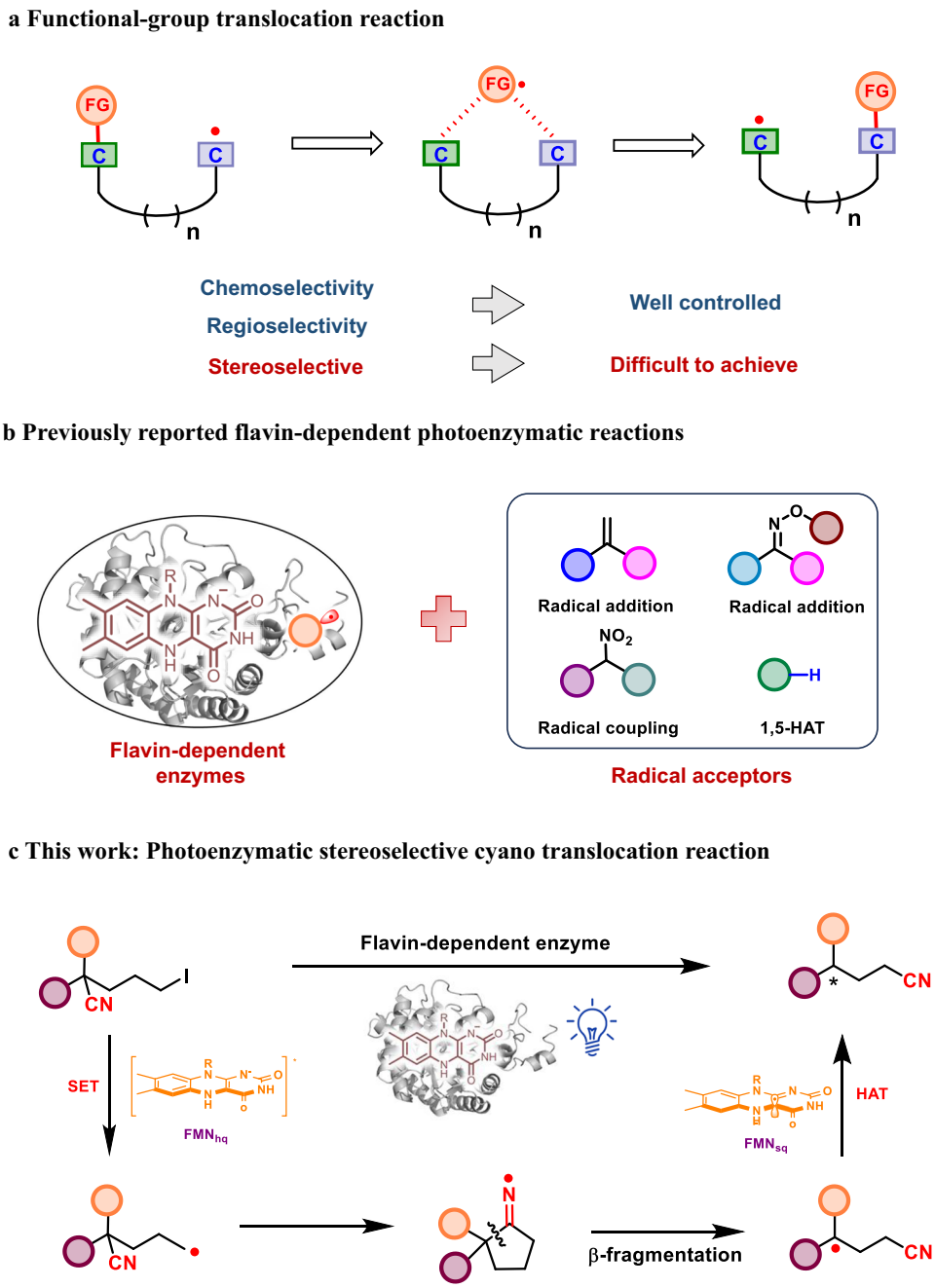

Fig. 1 | A Photoenzymatic strategy for functional-group translocation reaction. a Functional-group translocation reaction. **b** Previously reported flavin-dependent photoenzymatic reactions. **c** Photoenzymatic stereoselective cyano translocation reaction.

In this work, we selected CN translocation as a representative transformation. Inspired by chemical precedents, our design involves the generation of a neutral alkyl radical within the enzyme active site, which enables addition to the C≡N bond followed by β-fragmentation of the resulting iminyl radical to effect CN migration[7–9]. The ensuing radical is subsequently quenched via enzyme-catalyzed stereoselective hydrogen atom transfer (HAT), thereby providing access to chiral alkyl nitriles with high stereocontrol (Fig. 1c).

Results

The excited state of flavin hydroquinone (FMN_{hq}*) possesses a reduction potential of approximately −2.26 V vs SCE[53], which enables the reduction of alkyl iodides ($E_{red} \approx -2.19$ V vs SCE)[54]. This redox compatibility prompted us to select 5-iodo-2-methyl-2-phenylpentanenitrile **1a** as a model substrate to evaluate the feasibility of the CN translocation reaction. Initially, we screened a panel of flavin-dependent enzymes and found that several displayed measurable catalytic activities (Table 1). Among them, old yellow enzyme 1 from *Saccharomyces pastorianus* (OYE1) catalyzed the formation of the product in 30% yield with 43:57 (*S*:*R*) stereoselectivity, whereas old yellow enzyme 3 from *Saccharomyces cerevisiae* (OYE3) afforded a 27% yield with 45:55 e.r. The optimal result was achieved with Caulobacter segnis arene reductase from *Caulobacter segnis* (CsER), providing the *S*-configured product in 69% yield and 98:2 e.r. In contrast, enoate reductase from *Gluconobacter oxydans* (GluER) afforded the opposite stereoisomer in 57% yield with 1:99 e.r. Control experiments were then performed, as shown in Table 1, entry 5-8. No product was detected in the absence of the enzyme, GDH, or light, indicating that the transformation relies on the excited FMN_{hq}. When the enzymes were replaced with FMN alone, only trace amounts of product were formed

https://doi.org/10.1038/s41467-026-68776-8

Table 1 | Optimization for the photoenzymatic enantioselective CN translocation reaction

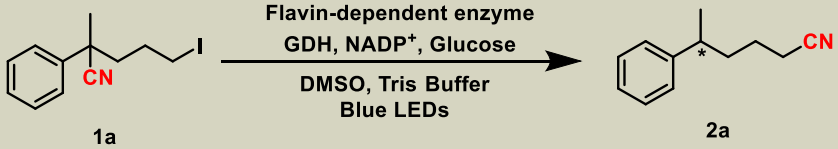

1a 2a

Entry	Enzyme	Change from standard conditions	Yield (%)	e.r. (S:R)
1	OYE1	none	30	43:57
2	OYE3	none	27	45:55
3	CsER	none	69	98:2
4	GluER	none	57	1:99
5	CsER	no enzyme	0	-
6	CsER	no GDH	<5	-
7	CsER	No Blue LEDs	0	-
8	CsER	FMN instead of enzyme	trace	-

Reaction conditions: **1a** (3 mM), Flavin-dependent enzyme (1 mol%), $NADP^+$ (0.1 μmol), GDH (0.1 mg, about 3 U), glucose (100 μmol), solvent (960 μL, 50 mM tris buffer, pH 8.0 and 40 μL DMSO), at room temperature with the irradiation Blue LEDs reaction for 12 h under N_2 atmosphere; Yield and enantiomeric ratio (e.r.) were determined by GC.

without stereoselectivity, highlighting the indispensable role of enzyme scaffold in orchestrating both reactivity and stereocontrol. While our manuscript was under revision, Yang reported a similar cyano migration reaction catalyzed by an NADPH-dependent imine reductase[55].

With the optimal reaction conditions in hand, we explored the substrate scope for this photoenzymatic CN translocation reaction. As shown in Fig. 2, substrates bearing either electron-rich (*S*)-**2b**-**2e** or electron-deficient substituents (*S*)-**2f**-**2g** on the phenyl ring were tolerated, delivering products with good reactivity and stereoselectivity. The disubstituted aromatic substrate **1e** was also efficiently converted into (*S*)-**2e** in 53% yield with 90:10 e.r. In addition to the benzyl-position methyl group, the ethyl-substituted substrate **1h** was evaluated, which afforded the corresponding product (*S*)-**2h** in 65% yield with 97:3 e.r. Furthermore, substrates bearing larger alkyl groups at benzyl position (R = *i*-Pr (**1i**) and Cy (**1j**)) were not well tolerated. Sterically demanding naphthyl substrate **1k** was accommodated in the reaction, affording product (*S*)-**2k** in 24% yield with 98:2 e.r. Compounds bearing heterocyclic substituents were well tolerated, affording the pyridine-substituted product (*S*)-**2l** in 65% yield with 99:1 e.r. and the thiophene-substituted product (*S*)-**2m** in 63% yield with 97:3 e.r. Benzyl-substituted substrates were further examined to expand the substrate scope. The dicyano-substituted benzyl derivative (**1n**) reacted with moderate yield and decreased stereoselectivity (Table S5). We further employed **1n** as a substrate to screen and evolve flavin-dependent enzymes, and identified OYE3-Y196F as the improved mutant, affording (*R*)-**2n** in 70% yield and 85:15 e.r. (Table S6). We hypothesize that the reduced stereoselectivity of these substrates may result from accelerated radical quenching facilitated by electron-withdrawing cyano groups. Consistent with this hypothesis, introducing electron-donating groups on the phenyl ring enhanced stereoselectivity((*R*)-**2o**, (*R*)-**2p** and (*R*)-**2q**), whereas electron-withdrawing groups further diminished it ((*R*)-**2t**: 85% yield, 70:30 e.r.), underscoring the critical role of electronic effects in governing stereocontrol. Benzyl ester-substituted substrate **1u** also underwent the reaction, providing the desired products (*R*)-**2u** in good yields with moderate stereoselectivity. Finally, we examined the reversed-selectivity reactions catalyzed by GluER, identified in the initial screening, and found that its substrate scope was highly limited ((*R*)-**2a**: 57% yield, 1:99 e.r.; (*R*)-**2f**: 35% yield, 14:86 e.r.). Finally, the scaled-up reaction (0.1 mmol of **1d**) was implemented, affording the corresponding product in 50% yield and 99:1 e.r.

To gain insight into the mechanism of this transformation, we carried out a series of control experiments. Radical trapping experiments employing TEMPO significantly suppressed the product yield (Fig. 3a) and enabled the detection of the corresponding TEMPO-substrate adduct (Section 5.2 in SI). This result suggests that the reaction proceeds via a radical pathway. Furthermore, the reaction maintained a yield of 32% even in the presence of TEMPO. This result likely stems from the generation of the alkyl radical intermediate within the confined enzyme pocket, where intramolecular CN trapping is more readily achieved than intermolecular quenching by TEMPO. UV–visible spectroscopy revealed that FMN_{hq} alone exhibits no absorption in the visible region, whereas the addition of the substrate induces the formation of a distinct Electron Donor-Acceptor (EDA) complex, enhancing the system's absorption under visible light (Fig. 3b). Experiments were conducted of alkene substrates (**1w** and **1v**) with different carbon-chain lengths. As shown in Fig. 3c, deiodinated products from direct hydrogen atom transfer (HAT) were detected, whereas no cyano migration products were observed (Section 5.5 in SI). To further probe the mechanistic basis of this observation, density functional theory (DFT) calculations were performed on cluster models composed of FMN_{sq} and the corresponding deiodinated radical intermediates (Fig. S15–S17). The results reveal that the 1,4-cyano translocation pathway of **1a**, proceeding via a five-membered cyclic radical intermediate, is energetically favored, in good agreement with the experimental observations. Isotopic labeling experiments were carried out to probe the reaction quenching pathway. No deuterium incorporation was observed in the product using a deuterated buffer. By contrast, in situ generation of deuterated flavin semiquinone (FMN_{sq}) from deuterated glucose led to 56% deuterium incorporation (Fig. 3d), supporting that quenching occurs via FMN_{sq}.

To elucidate the origin of stereoselectivity in this new-to-nature enzymatic reaction at the molecular level, molecular dynamics (MD) simulations were conducted. As the final HAT process determined the stereoselectivity of products, we focused on the stage that the β-fragmentation of the iminyl radical has achieved, with the cofactor under the FMN_{sq} state (Fig. 3e). The RMSD profiles of all binding components and the key distance between the HAT involved atoms, i.e., H5 of FMN_{sq} and C7 of **2a**$^{\bullet}$, became converged within 200 ns.

https://doi.org/10.1038/s41467-026-68776-8

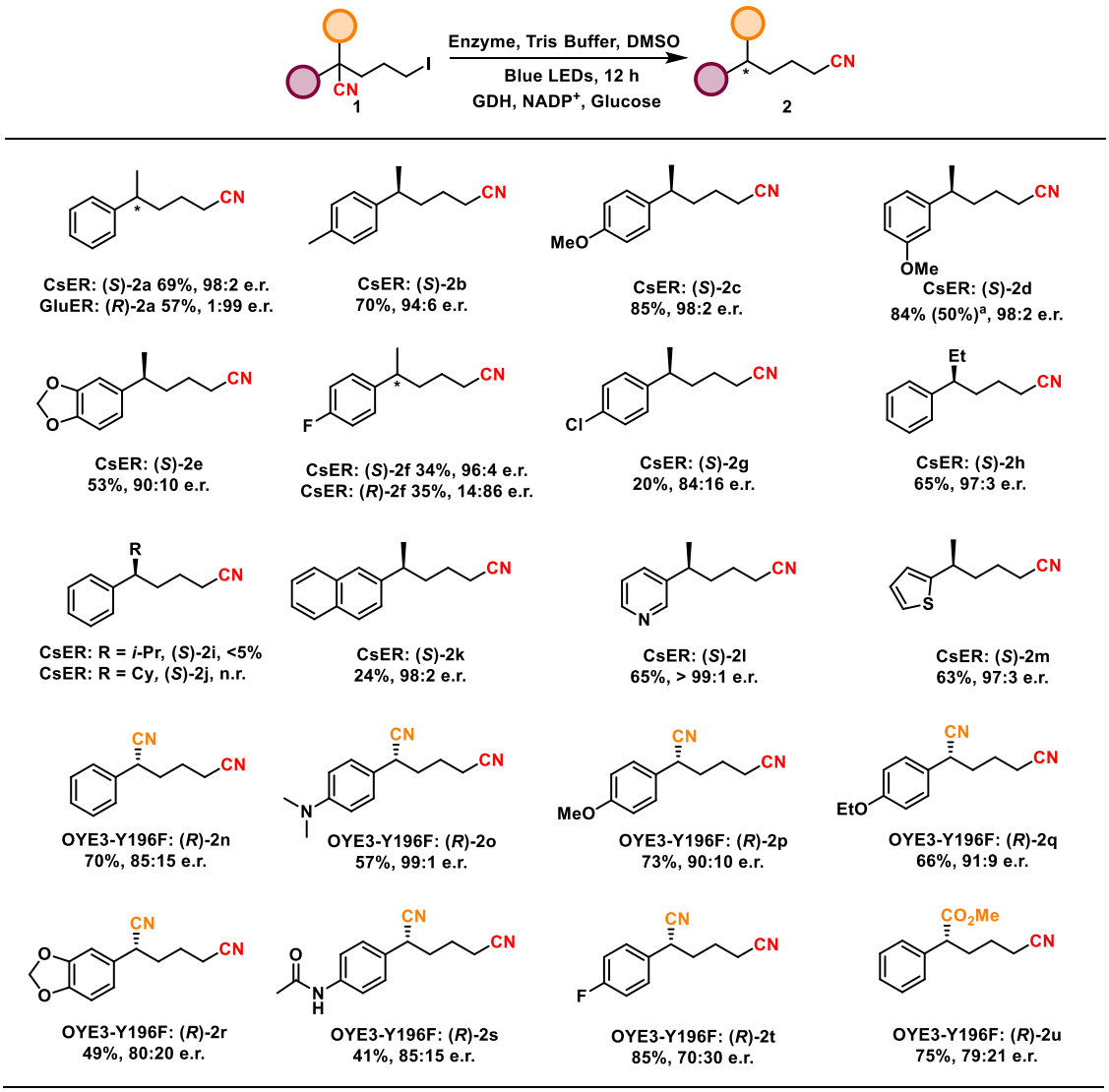

Fig. 2 | Substrate scope of the photoenzymatic enantioselective CN translocation reaction. The reaction conditions of **1a**-**1m**: **1a**-**1m** (3 mM), CsER (1 mol%), $NADP^+$ (0.1 μmol), GDH (0.1 mg, about 3 U), glucose (100 μmol), solvent (960 μL, 50 mM tris buffer, pH 8.0 and 40 μL DMSO), at room temperature with the irradiation Blue LEDs reaction for 12 h under N_2 atmosphere; The reaction conditions of **1a** and **1f**: **1a** or **1f** (3 mM), GluER (1 mol%), $NADP^+$ (0.1 μmol), GDH (0.1 mg, about 3 U), glucose (100 μmol), solvent (960 μL, 50 mM tris buffer, pH 8.0 and 40 μL DMSO), at room temperature with the irradiation Blue LEDs reaction for 12 h under N_2 atmosphere; The reaction conditions of **1n**-**1u**: **1n**-**1u** (3 mM), OYE3-Y196F (1 mol%), $NADP^+$ (0.1 μmol), GDH (0.1 mg, about 3 U), glucose (100 μmol), solvent (960 μL, 50 mM KPi buffer, pH 8.0 and 40 μL CH_3CN), at room temperature with the irradiation Blue LEDs reaction for 12 h under N_2 atmosphere; a, Isolated yield based on a 0.1-mmol reaction. Yield were determined by HPLC and enantiomeric ratio (e.r.) were determined by GC or HPLC.

However, the dihedral formed by the coplanar C3, C8, and C7 of **2a**• and the H5 of FMN_{sq} (∠C3-C8-C7-H5), an indicator of the hydrogen atom incorporation via a *re* or *si* face, showed a highly biased distribution (Figs. S4 and S5), which agrees well with the experimentally determined e.r values. The representative binding conformations demonstrated consistent binding features. The cyano group of **2a**• anchored to a polar environment built mainly by the H173/H172 and N176/N175 sidechains in CsER/GluER in almost all cases. Relative to the pro-(*R*) binding form, the benzyl group of pro-(*S*) **2a**• formed additional parallel π-π stacking interactions with Y66 (Fig. S8), providing extra binding stability. In binding with GluER, two π-π stacking interactions were observed for both the pro-(*R*) (with W66 and W342) and pro-(*S*) (with W66 and F269) **2a**•. However, the distances of the pro-(*S*) **2a**• involved π-π stacking are relatively longer than that of the pro-(*R*) **2a**• (Fig. 3e and Fig. S10), indicating a decreased binding strength. For the dicyano-substituted inetermediate **2n**•, a distinct binding feature was discovered in its binding with OYE3 (Y196F), i.e., the H5 atom is almost always coplanar with the radical plane of **2n**• (defined by atoms C3, C7, and C8, Fig. S7), leading to a concentrated distribution of dihedral angles around 180° and −180° and a decreased conformational preference (Fig. S6). In comparison with the pro-(*S*) **2n**•, the pro-(*R*) binding form is more favorable by forming a sandwich framework with Y82 and Y375 through π-π stacking interactions, resulting in a dihedral distribution which is in accordance with the stereoselectivity of OYE3 (Y196F) (Figs. S6 and S7). Notably, with the cyano group of **2a**•/**2n**• stably anchored to the polar residues His and/or Asn through hydrogen bond interactions in all binding systems, the prochiral conversion can be primarily attributed to the rotation of the C7–C8 bond. Together, MD simulations shed light on the mechanism of stereoselective cyano translocation.

Discussion

In summary, we report a flavin-dependent, photoenzymatic method for the stereoselective translocation of cyano groups. Previous studies have

https://doi.org/10.1038/s41467-026-68776-8

a Radical capture experiment

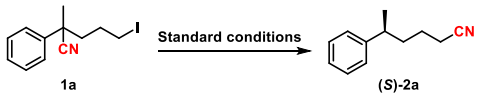

Entry	Conditions	Yield of (*S*)-2a
1	Standard conditions	69%
2	TEMPO (4 equiv)	32%

b UV-visible spectroscopic analysis

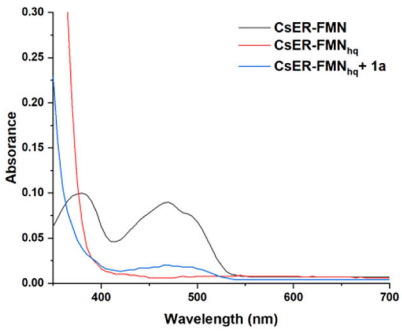

c Cyano translocation of 1 with different chain lengths

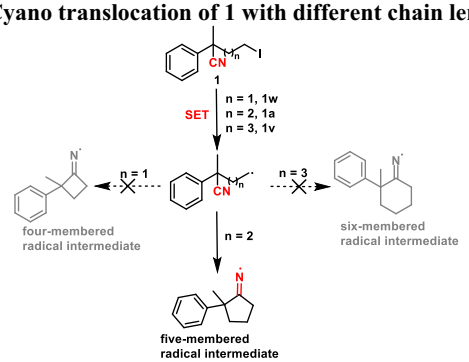

d Deuterium incorporation experiments

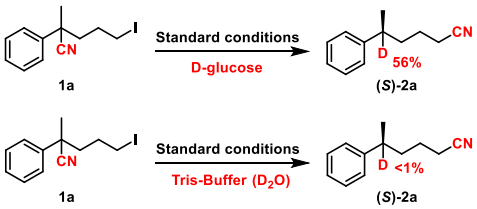

e Molecular dynamics (MD) simulations

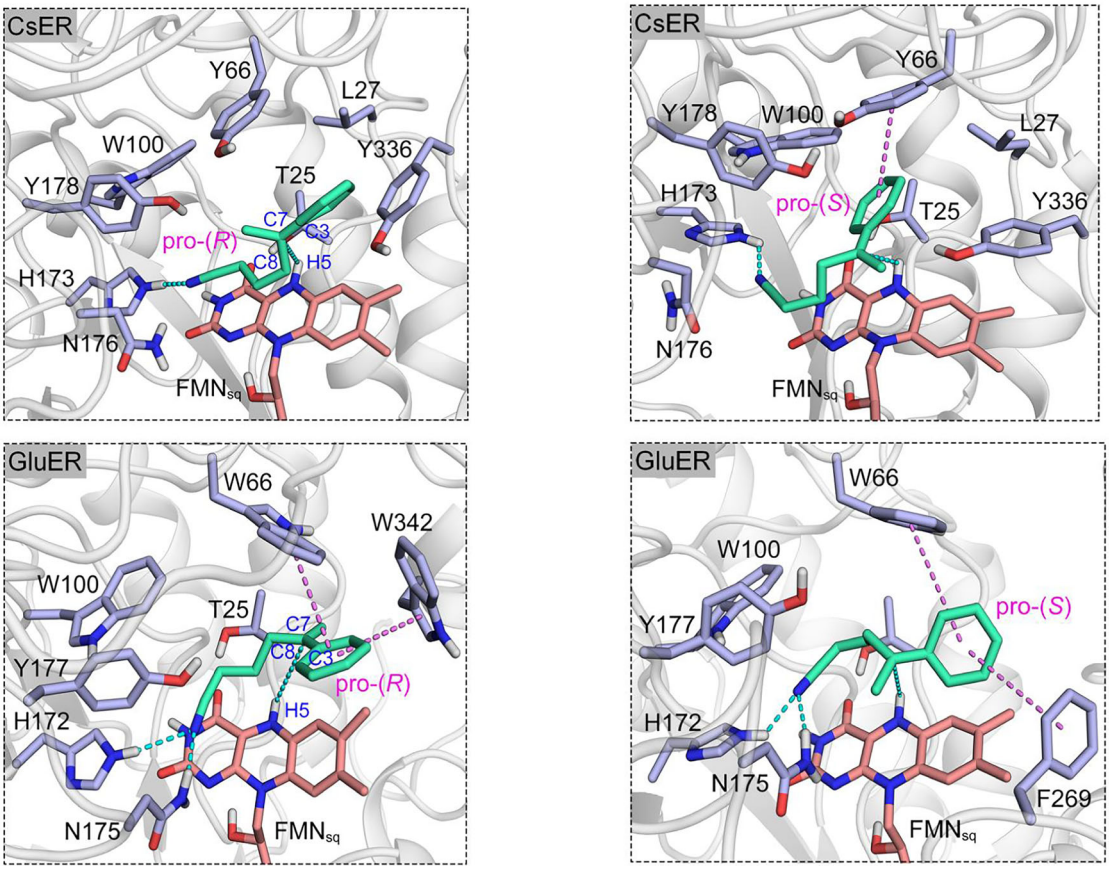

Fig. 3 | Mechanistic studies. a Radical capture experiment. **b** UV-visible spectroscopic analysis. **c** 1,5-functional group migration. **d** Deuterium incorporation experiments. **e** Molecular dynamics (MD) simulations: Representative binding conformations of CsER/GluER and the intermediate radical **2a•** chosen based on k-means clustering analysis of the MD trajectories. The atoms defining the dihedral angle ∠C3-C8-C7-H5 were labeled. Key distances were indicated with cyan dotted lines. The π-π stacking interactions were indicated as pink dotted lines.

rarely addressed the stereocontrol of functional group translocation reactions. Here, we exploit the stereoselective HAT of FMN_{sq} within the active site of flavin-dependent enzymes to achieve precise control over reaction selectivity. Moreover, computational studies provide insight into the origin of the observed stereoselectivity. This study not only establishes a new paradigm for photoenzymatic catalysis but also offers a solution to a remaining challenge in organic synthesis.

Methods

Flavin-dependent enzyme catalyzed cyano translocation reaction

960 μL Enzyme solution (0.025–0.03 μmol pure enzyme, 1 mol%, tris buffer, pH = 8.0) contain $NADP^+$ (7 μL, 0.1 μmol, 15 mM stock in buffer, 3 mol%), GDH (100 μL, about 3 U, 30 U/mL stock in buffer), glucose (100 μmol, 33.3 equiv) was added to a 10 mL Schlenk tube containing a magnetic stir bar. **1** (3 μmol, 1.0 equiv) in DMSO (40 μL) was following added into the system. The mixture was then degassed by freeze-pump-thaw for three times under N_2 atmosphere. The reaction was stirred for 12 h at room temperature. Then the reaction was extracted by ethyl acetate for three times (1 mL × 3). The enantioselectivity was determined by GC or HPLC.

Reporting summary

Further information on research design is available in the Nature Portfolio Reporting Summary linked to this article.

Data availability

Data relating to the materials and methods, experimental procedures, mechanistic studies and computational calculations, gas chromatography, high-performance liquid chromatography spectra and NMR spectra are available in the Supplementary Information and from the corresponding authors upon request.

References

1. Sweeney, J. B. Molecular rearrangements in organic synthesis. Edited by Christian M. Rojas. *Angew. Chem. Int. Ed.* **55**, 13928–13928 (2016).
2. Sommer, H., Juliá-Hernández, F., Martin, R. & Marek, I. Walking metals for remote functionalization. *ACS Cent. Sci.* **4**, 153–165 (2018).
3. Gat, S. N., Pattanaik, P. P. & Dandela, R. Recent developments in organic synthesis for constructing carbon frameworks using transposition strategies. *Org. Chem. Front.* **12**, 4151–4180 (2025).
4. Studer, A. & Bossart, M. Radical aryl migration reactions. *Tetrahedron* **57**, 9649–9667 (2001).
5. Robertson, J., Pillai, J. & Lush, R. K. Radical translocation reactions in synthesis. *Chem. Soc. Rev.* **30**, 94–103 (2001).
6. Chen, Z.-M., Zhang, X.-M. & Tu, Y.-Q. Radical aryl migration reactions and synthetic applications. *Chem. Soc. Rev.* **44**, 5220–5245 (2015).
7. Li, W., Xu, W., Xie, J., Yu, S. & Zhu, C. Distal radical migration strategy: an emerging synthetic means. *Chem. Soc. Rev.* **47**, 654–667 (2018).
8. Wu, X. & Zhu, C. Radical-mediated remote functional group migration. *Acc. Chem. Res.* **53**, 1620–1636 (2020).
9. Wu, X., Ma, Z., Feng, T. & Zhu, C. Radical-mediated rearrangements: past, present, and future. *Chem. Soc. Rev.* **50**, 11577–11613 (2021).
10. Chen, K. et al. Functional-group translocation of cyano groups by reversible C–H sampling. *Nature* **620**, 1007–1012 (2023).
11. Li, L., Yu, T., Du, K. & Xu, P. Cyano group translocation to alkenyl C(Sp^2)–H site by radical cation catalysis. *Nat. Commun.* **16**, 7251 (2025).
12. Chen, F., Cao, Z. & Zhu, C. Asymmetric functionalization harnessing radical-mediated functional-group migration. *Angew. Chem. Int. Ed.* **64**, e202424667 (2025).
13. Reetz, M. T. Biocatalysis in organic chemistry and biotechnology: past, present, and future. *J. Am. Chem. Soc.* **135**, 12480–12496 (2013).
14. Carvalho, M. F. & Oliveira, R. S. Natural production of fluorinated compounds and biotechnological prospects of the fluorinase enzyme. *Crit. Rev. Biotechnol.* **37**, 880–897 (2017).
15. Schwizer, F. et al. Artificial metalloenzymes: reaction scope and optimization strategies. *Chem. Rev.* **118**, 142–231 (2018).
16. Zeymer, C. & Hilvert, D. Directed evolution of protein catalysts. *Annu. Rev. Biochem.* **87**, 131–157 (2018).
17. Devine, P. N. et al. Extending the application of biocatalysis to meet the challenges of drug development. *Nat. Rev. Chem.* **2**, 409–421 (2018).
18. Leveson-Gower, R. B., Mayer, C. & Roelfes, G. The importance of catalytic promiscuity for enzyme design and evolution. *Nat. Rev. Chem.* **3**, 687–705 (2019).
19. Chen, K. & Arnold, F. H. Engineering new catalytic activities in enzymes. *Nat. Catal.* **3**, 203–213 (2020).
20. Hollmann, F., Opperman, D. J. & Paul, C. E. Biocatalytic reduction reactions from a chemist's perspective. *Angew. Chem. Int. Ed.* **60**, 5644–5665 (2021).
21. Buller, R. et al. From nature to industry: harnessing enzymes for biocatalysis. *Science* **382**, eadh8615 (2023).
22. Xu, Y., Liu, F., Zhao, B. & Huang, X. Repurposing naturally occurring enzymes using visible light. *Chin. J. Chem.* **42**, 3553–3558 (2024).
23. Kan, S. B. J., Lewis, R. D., Chen, K. & Arnold, F. H. Directed evolution of cytochrome c for carbon–silicon bond formation: bringing silicon to life. *Science* **354**, 1048–1051 (2016).
24. Prier, C. K., Zhang, R. K., Buller, A. R., Brinkmann-Chen, S. & Arnold, F. H. Enantioselective, intermolecular benzylic C–H amination catalysed by an engineered iron-haem enzyme. *Nat. Chem.* **9**, 629–634 (2017).
25. Zhang, R. K. et al. Enzymatic assembly of carbon–carbon bonds via iron-catalysed Sp^3 C–H functionalization. *Nature* **565**, 67–72 (2019).
26. Yang, Y., Cho, I., Qi, X., Liu, P. & Arnold, F. H. An enzymatic platform for the asymmetric amination of primary, secondary and tertiary C(Sp^3)–H bonds. *Nat. Chem.* **11**, 987–993 (2019).
27. Zhou, Q., Chin, M., Fu, Y., Liu, P. & Yang, Y. Stereodivergent atom-transfer radical cyclization by engineered cytochromes P450. *Science* **374**, 1612–1616 (2021).
28. Roy, S. et al. Stereoselective construction of β-, γ- and δ-lactam rings via enzymatic C–H amidation. *Nat. Catal.* **7**, 65–76 (2023).
29. Romero, E., Gómez Castellanos, J. R., Gadda, G., Fraaije, M. W. & Mattevi, A. Same substrate, many reactions: oxygen activation in flavoenzymes. *Chem. Rev.* **118**, 1742–1769 (2018).
30. Hall, M. Flavoenzymes for biocatalysis. *Enzymes*, **47**, 37–62 (2020).
31. Harrison, W., Huang, X. & Zhao, H. Photobiocatalysis for abiological transformations. *Acc. Chem. Res.* **55**, 1087–1096 (2022).
32. Emmanuel, M. A. et al. Photobiocatalytic strategies for organic synthesis. *Chem. Rev.* **123**, 5459–5520 (2023).
33. Fu, H. & Hyster, T. K. From ground-state to excited-state activation modes: flavin-dependent "ene"-reductases catalyzed non-natural radical reactions. *Acc. Chem. Res.* **57**, 1446–1457 (2024).
34. Yang, X. et al. Bridging chemistry and biology for light-driven new-to-nature enantioselective photoenzymatic catalysis. *Chem. Soc. Rev.* **54**, 5157–5188 (2025).
35. Yu, J., Chen, B. & Huang, X. Single-electron oxidation triggered by visible-light-excited enzymes for asymmetric biocatalysis. *Angew. Chem. Int. Ed.* **64**, e202419262 (2025).
36. Zeng, Q.-Q. et al. Biocatalytic desymmetrization for synthesis of chiral enones using flavoenzymes. *Nat. Synth.* **3**, 1340–1348 (2024).
37. Wang, H. et al. Unmasking the reverse catalytic activity of 'ene'-reductases for asymmetric carbonyl desaturation. *Nat. Chem.* **17**, 74–82 (2025).

38. Biegasiewicz, K. F. et al. Photoexcitation of flavoenzymes enables a stereoselective radical cyclization. *Science* **364**, 1166–1169 (2019).
39. Huang, X. et al. Photoenzymatic enantioselective intermolecular radical hydroalkylation. *Nature* **584**, 69–74 (2020).
40. Sorigué, D. et al. Mechanism and dynamics of fatty acid photodecarboxylase. *Science* **372**, eabd5687 (2021).
41. Fu, H. et al. An asymmetric Sp^3–Sp^3 cross-electrophile coupling using 'ene'-reductases. *Nature* **610**, 302–307 (2022).
42. Zhao, B. et al. Direct visible-light-excited flavoproteins for redox-neutral asymmetric radical hydroarylation. *Nat. Catal.* **6**, 996–1004 (2023).
43. Chen, X. et al. Photoenzymatic hydrosulfonylation for the stereoselective synthesis of chiral sulfones. *Angew. Chem. Int. Ed.* **62**, e202218140 (2023).
44. Xu, W. et al. Catalytic promiscuity of fatty acid photodecarboxylase enables stereoselective synthesis of chiral α-tetralones. *Angew. Chem. Int. Ed.* **63**, e202412862 (2024).
45. Shi, Q. et al. Single-electron oxidation-initiated enantioselective hydrosulfonylation of olefins enabled by photoenzymatic catalysis. *J. Am. Chem. Soc.* **146**, 2748–2756 (2024).
46. Ju, S. et al. Stereodivergent photobiocatalytic radical cyclization through the repurposing and directed evolution of fatty acid photodecarboxylases. *Nat. Chem.* **16**, 1339–1347 (2024).
47. Wu, D. et al. Cooperative photoenzymatic catalysis for enantioselective fluoroalkylation/cyclization cascade. *J. Am. Chem. Soc.* **147**, 25508–25516 (2025).
48. Gao, X. et al. Photoenzymatic synthesis of α-tertiary amines by engineered flavin-dependent "ene"-reductases. *J. Am. Chem. Soc.* **143**, 19643–19647 (2021).
49. Zhang, Z. et al. Photoenzymatic stereoablative enantioconvergence of γ-chiral oximes via hydrogen atom transfer. *Nat. Catal.* **8**, 548–555 (2025).
50. Sruthi, P. R. & Anas, S. An overview of synthetic modification of nitrile group in polymers and applications. *J. Polym. Sci.* **58**, 1039–1061 (2020).
51. Xia, Y., Jiang, H. & Wu, W. Recent advances in chemical modifications of nitriles. *Eur. J. Org. Chem.* **2021**, 6658–6669 (2021).
52. Rakshit, A., Dhara, H. N., Sahoo, A. K. & Patel, B. K. The renaissance of organo nitriles in organic synthesis. *Chem. Asian J.* **17**, e202200792 (2022).
53. Warren, J. J., Ener, M. E., Vlček, A., Winkler, J. R. & Gray, H. B. Electron hopping through proteins. *Coord. Chem. Rev.* **256**, 2478–2487 (2012).
54. Clayman, P. D. & Hyster, T. K. Photoenzymatic generation of unstabilized alkyl radicals: an asymmetric reductive cyclization. *J. Am. Chem. Soc.* **142**, 15673–15677 (2020).
55. Liu, A. & Yang, Y. Imine reductase-catalyzed, radical-mediated asymmetric cyano group migration. *J. Am. Chem. Soc.* **147**, 43604–43611 (2025).

Acknowledgements

This research was funded by National Natural Science Foundation of China (No. 22322705, 22171243, 22301276), Zhejiang Provincial Natural Science Foundation of China (LQ24B020009), Fundamental Research Funds for the Provincial Universities of Zhejiang (No. RF-C2024003, RF-A2025013). The authors thanks Mr. Jiahui Xu from Analysis and Testing Center at Zhejiang University of Technology for the supporting in NMR measurements. This study was supported by Advanced Computation Center of Hangzhou Normal University.

Author contributions

J.X. conceived the project. J.X. and X.D. directed the project. X.D., J.X. and R.B. developed the reactions and performed the majority of synthetic experiments. C.J., Y.C., G.W., and L.P. assisted with synthetic experiments. Z.W. conducted computational studies. J.X., X.D. and C.Y. wrote the paper with input from all authors.

Competing interests

The authors declare no competing interests.

Additional information

Supplementary information The online version contains supplementary material available at https://doi.org/10.1038/s41467-026-68776-8.

Correspondence and requests for materials should be addressed to Chunlei Yang, Zhiguo Wang or Jian Xu.

Peer review information *Nature Communications* thanks anonymous reviewers for their contribution to the peer review of this work.